Published in final edited form as:
Free Radic Biol Med. 2007 April 1; 42(7): 1049–1061. doi:10.1016/j.freeradbiomed.2007.01.005.

Hydrogen Peroxide Induces Nitric Oxide and Proteosome Activity in Endothelial Cells: A Bell-Shaped Signaling Response

Simmy Thomas[a,b], **Srigiridhar Kotamraju**[a,b], **Jacek Zielonka**[a,b], **David R. Harder**[b,c], and **B. Kalyanaraman**[a,b]

a *Department of Biophysics, Medical College of Wisconsin, 8701 Watertown Plank Road, Milwaukee, WI, 53226 USA*

b *Free Radical Research Center, Medical College of Wisconsin, 8701 Watertown Plank Road, Milwaukee, WI, 53226 USA*

c *Cardiovascular Research Center, Medical College of Wisconsin, 8701 Watertown Plank Road, Milwaukee, WI, 53226 USA, 414-456-4000 (phone), 414-456-6512 (fax), balarama@mcw.edu*

Abstract

We investigated nitric oxide ($^{\bullet}NO$)-mediated proteosomal activation in bovine aortic endothelial cells (BAEC) treated with varying fluxes of hydrogen peroxide (H_2O_2) generated from glucose/glucose oxidase (Glu/GO). Results revealed a bell-shaped $^{\bullet}NO$ signaling response in BAEC treated with Glu/GO (2–20 mU/ml). GO treatment (2 mU/ml) enhanced eNOS phosphorylation and $^{\bullet}NO$ release in BAEC. With increasing GO concentrations, phospho eNOS and $^{\bullet}NO$ levels decreased. A bell-shaped response in proteasomal function and $^{\bullet}NO$ induction was observed in BAEC treated with varying levels of GO (2–10 mU/ml). Proteosomal activation induced in GO-treated BAEC was inhibited by L-NAME pretreatment, suggesting that $^{\bullet}NO$ mediates proteasomal activation. Intracellular $^{\bullet}NO$ induced by H_2O_2 was detected by isolating the DAF-2/$^{\bullet}NO/O_2$-derived "green fluorescent product" using the HPLC-fluorescence technique, a more rigorous and quantitative methodology for detecting the DAF-2/$^{\bullet}NO/O_2$ reaction product. Finally, the relationship between H_2O_2 flux, proteasomal activation/inactivation and endothelial cell survival and apoptosis is discussed.

Keywords

hydrogen peroxide; nitric oxide; proteasome activation; apoptosis; diaminofluorescein; DAF-2; HPLC

Introduction

The chemical biology of the reactive oxygen species (ROS) (e.g., superoxide, hydrogen peroxide) and their signal transduction mechanisms in physiological and pathophysiological processes are complex, intriguing and continuously evolving [1–5]. Hydrogen peroxide (H_2O_2) is generated in most mammalian cells as a byproduct of oxygen metabolism. Low levels of ROS generation can stimulate cell growth and cell proliferation [6–8]. However, excessive

Address correspondence and reprint requests to: B. Kalyanaraman, Ph.D., Department of Biophysics and Free Radical Research Center, Medical College of Wisconsin, 8701 Watertown Plank Road, Milwaukee, WI, 53226 USA, E-mail: balarama@mcw.edu.

generation of ROS under pathophysiological conditions (inflammation, cardiovascular and neurodegenerative disorders) can induce cell injury due to oxidative damage to lipid membranes, proteins and DNA. Thus, there is a great deal of interest in research pertaining to the regulation of antioxidant enzymes (superoxide dismutases and peroxidases) and other processes (proteasomal activation and ubiquitinylation) that are responsible for repairing oxidatively-damaged lipids, protein, and DNA [9,10]. H_2O_2 has been suggested to be a "second messenger" in redox-signaling events [11,12]. Recent research suggests that H_2O_2 can stimulate calcium, $^{\bullet}NO$, and cGMP/cAMP signaling in vascular endothelial and smooth muscle cells [13,14]. Emerging research indicate that $^{\bullet}NO$/cGMP/cAMP pathway is responsible for upregulating the proteasomal signaling mechanism in endothelial cells [15]. The proteasomal machinery serves an important antioxidant function in repairing oxidatively damaged proteins and lipids [10]. Thus, it is important to understand oxidant-induced regulation of the proteasomal function.

Endothelial injury is an early oxidative injury in several vascular diseases [16–18]. Endothelial cells are exposed to H_2O_2 and other lipid peroxides originating from shear stress and from leukocytes and macrophages [19,20]. The mechanism(s) by which peroxides induce endothelial dysfunction are not fully understood [3,21]. H_2O_2 induces transcriptional activation of eNOS in endothelial cells [5,13,22,23]. The cytoprotective effects of $^{\bullet}NO$ against H_2O_2-mediated cellular toxicity have been attributed to iron chelation, radical scavenging or restoration of mitochondrial respiration [24–26]. At higher concentrations of H_2O_2, the "uncoupling" of eNOS was reported to stimulate additional superoxide formation [27]. To more fully define the peroxide-mediated downstream signaling pathway, we investigated the dose-response relationship between H_2O_2, $^{\bullet}NO$ formation and proteasomal activation in BAEC treated with glucose/glucose oxidase (Glu/GO).

The present results suggest that H_2O_2 stimulates a bell-shaped, $^{\bullet}NO$ -mediated proteasomal signaling response in endothelial cells. At low levels of H_2O_2, there was an increase in $^{\bullet}NO$ signaling. This signaling mechanism was abolished in cells treated with higher concentrations of H_2O_2. The present data reveal a new mechanistic perspective in the oxidant-induced regulation of signal transduction processes involved in cell survival and cell death. In addition, we have described in this study a HPLC-fluorescence methodology to detect and unambiguously quantitate the DAF-2/$^{\bullet}NO/O_2$-derived fluorescent product. The formation of DAf-2 triazole product, as detected by HPLC-fluorescence, is more sensitive to NOS inhibitors as compared to optical microscope technique.

Materials and Methods

Materials

Glucose oxidase, clasto-lactacystin-β-lactone, N_{ω}-Nitro-L-arginine-methyl ester (L-NAME) and N^G-monomethyl-L-arginine monoacetate (L-NMMA) were obtained from Sigma Chemical Co (St. Louis, MO). 4,5-Diaminofluorescein (DAF-2), DAF-2 diacetate (DAF-2DA) and DAF-2-triazole (DAF-2T) were purchased from Calbiochem (San Diego CA). The polyclonal antibodies directed against phospho-eNOS (Ser1177), Akt, and phospho-Akt (Ser473) were purchased from Cell Signaling Technology (Beverly, MA). Cell culture reagents including L-glutamine, penicillin, streptomycin and fetal bovine serum (FBS) were obtained from Invitrogen (Carlsbad, CA). All other chemicals used were of analytical grade.

Endothelial cell culture

Bovine aortic endothelial cells (BAEC) were obtained from Clonetics (San Diego, CA) and maintained (37°C, 5% CO_2) in Dulbecco's modified Eagle's medium (DMEM) containing 10% FBS, L-glutamine (4 mM), penicillin (100 units/ml), streptomycin (100 μg/ml) and

glucose (25 mM). Cells were obtained between passages 2 and 10. One day before treatment the medium was replaced with DMEM containing 2% FBS. GO (1–20 mU/ml) was added to cells in the medium containing 25 mM Glu. H_2O_2 (1 μM/min) was generated from Glu/GO (20 mU/ml) in 10 ml DMEM containing 2% FBS, and this was measured by using a YSI Model 25 oxidase meter (Yellow Springs Instruments). Nitric oxide synthase inhibitors [L-NAME (2 mM) and L-NMMA (200 μM)] and proteasome inhibitor [lactacystin-β-lactone (10 μM)], were added 2 h before GO treatment.

Intracellular conversion of 3-(4,5-dimethylthiazol-2-yl)-2,5-diphenyltetrazolium bromide (MTT) to formazan was used as an indicator of cell viability (λ_{max} = 562 nm). After treatment with H_2O_2, the culture media were removed, and cells were washed twice with Dulbecco's phosphate-buffered saline (DPBS). Cells were incubated with the culture medium (DMEM) alone without FBS containing 0.25 mg/ml MTT for 1 h at 37°C. Following this, the medium was removed. Cells were washed again with DPBS and finally dissolved in dimethyl sulfoxide (DMSO). The amount of formazan formed was measured spectrophotometrically as described previously [28].

Measurement of caspase-3 activity

The cytosolic enzymatic activity of caspase-3 was measured as described previously [29]. Briefly, cells were washed twice with DPBS following treatment with H_2O_2 and then lysed with 50 mM HEPES buffer (pH 7.4) containing 5 mM CHAPS and 5 mM dithiothreitol. After removing the cytosolic fraction by centrifugation at 12,000 × *g* for 30 min, the activity of caspase-3 was measured using the substrates of ac-DEVD-*p*NA (acetyl-Asp-Glu-Val-Asp-*p*-nitroanilide). The absorbance at 405 nm of the released *p*NA was monitored in a spectrophotometer and quantitated using a *p*NA standard.

Measurement of apoptosis by TUNEL assay

The terminal deoxynucleotidyl transferase-mediated nick-end labeling (TUNEL) assay was used for microscopic detection of apoptosis [30]. This assay is based on labeling of 3′-free hydroxyl ends of the fragmented DNA with fluorescein-dUTP catalyzed by terminal deoxynucleotidyl transferase. Procedures were followed according to a commercially available kit (ApoAlert) from Clontech. Apoptotic cells exhibit a strong nuclear green fluorescence that can be detected using a standard fluorescein filter (520 nm). All cells stained with propidium iodide exhibit a strong red cytoplasmic fluorescence at 620 nm. The areas of apoptotic cells were detected by fluorescence microscopy equipped with rhodamine and FITC filters. The quantification of apoptosis was performed using the Metamorph image analysis package.

Western blot analysis

BAEC were washed with ice-cold phosphate buffered saline (PBS) and homogenized in 100 μl of radioimmunoprecipitation assay buffer (20 mM Tris·HCl, pH 7.4/2.5 mM EDTA/1% Triton X-100/1% sodium deoxycholate/1% SDS/100 mM NaCl/100 mM sodium fluoride) containing 1 mM sodium *ortho*-vanadate and a mixture of protease inhibitors. The homogenate was centrifuged at 750 × *g* for 10 min at 4°C to pellet out the nuclei. The remaining supernatant was centrifuged for 30 min at 12,000 × *g*. Proteins were resolved on 8% for TfR, eNOS, phospho eNOS, Akt and phospho Akt by SDS/PAGE gels and blotted onto nitrocellulose membranes. Membranes were probed with primary antibodies and then incubated with horseradish peroxidase-conjugated rabbit anti-mouse IgG secondary antibody. Protein bands were detected by using the ECL method (Amersham Pharmacia).

Measurement of intracellular •NO

Intracellular •NO levels were monitored using the DAF-2 fluorescence probe [31,32]. The treated cells were washed with DPBS and incubated in 2 ml of fresh culture medium without FBS. DAF-2 was added at a final concentration of 5 μM, and the cells were incubated for 1 hr. The cells were washed twice with DPBS and maintained in 1 ml of culture medium. Fluorescence was monitored using a Nikon fluorescence microscope (excitation, 488 nm; emission, 610 nm) equipped with an FITC filter. The values of fluorescent intensity were calculated using the Metamorph software.

HPLC method

The HPLC method to detect intracellular •NO is more quantitative and specific, as DAF-2T (the product of •NO/O_2 and DAF-2) can be readily isolated and its concentration determined by comparison with an authentic standard. BAEC were treated with different concentrations of GO before incubation with DAF-2DA. Cells were subsequently washed twice with DPBS and treated with 5 μM DAF-2DA for 1 hr in DMEM medium containing 2% FBS. The medium was removed and cells were washed twice with DPBS and then harvested with DPBS. After centrifugation (5 min × 4,000 rpm) and removal of supernatant liquid, the pellets were stored at −80°C until the day of analysis by HPLC. On the day of analysis, the pellets were thawed to an ambient temperature and cells were lysed with 250 μl of phosphate buffer (10 mM, pH 7.5) containing 100 μM diethylenetriaminepentaacetic acid (DTPA) and 0.1% Triton X 100. Lysates (5 μl) were taken for protein measurement. To the remaining solution, 1-butanol (0.5 ml) was added and the mixture was vortexed for 10 min and then centrifuged (2 min × 5,000 rpm). An aliquot (450 μl) from n-butanol phase (upper layer) was separated and dried in a MultiVap analytical evaporator (Organomation) at 30°C using air flow. The dried samples were reconstituted in 50 μl of phosphate buffer (10 mM) containing 100 μM DTPA and used for HPLC analysis.

DAF-2, DAF-2T and other DAF-2DA - derived products (Fig. 1S in Supplementary Information) were separated on an Agilent 1100 HPLC system equipped with fluorescence and UV-Vis absorption detectors. Typically, 10 μl of sample was injected into the HPLC system with a C_{18} column (Agilent, Zorbax 80Å, Extend-C18, 4.6 × 250 mm, 5 μm) equipped with a guard column. The compounds of interest were separated by isocratic elution using an aqueous mobile phase consisting of potassium phosphate buffer pH 7.5 (10 mM) and acetonitrile (5% by volume) at a flow rate of 1 ml/min. Fluorescence detection at 490 nm (excitation) and 515 nm (emission) and absorbance changes at 220, 250, 280, 320, 490 nm were used to monitor the products.

Nitrate measurement

Nitrate, an oxidative metabolite of •NO, was measured by chemiluminescence according to a modified method [33]. Briefly, after treatment of BAEC with GO, the culture medium was collected, and the released nitrate was detected using the •NO analyzer. Protein concentration in each well was measured according to the Bradford method. For nitrate measurement, a solution containing vanadium and HCl was used. •NO generated from sodium nitrate was used as standard.

26S proteasome activity

Proteasome function was measured as reported [34,35]. Briefly, cells were washed with buffer I (50 mM Tris, pH 7.4/2 mM DTT/5 mM $MgCl_2$/2 mM ATP) after treatment, and homogenized with buffer I containing 250 mM sucrose. Twenty micrograms of 10,000 × *g* supernatant were diluted with buffer I to a final volume of 900 μl. The fluorogenic proteasome substrates SucLLVY-AMC (chymotrypsin-like) and Z-Leu-Leu-Lys-AMC (trypsin-like) were added in

a final concentration of 80 μM. Proteolytic activity was measured by monitoring the release of the fluorescent group 7-amido-4-methylcoumarin (excitation 380 nm, emission 460 nm).

20S proteasome activity

Activity of the 20S proteasome was determined according to Grune *et al.* (36). Cells were lysed in PBS containing 0.1% Triton X-100 and 0.5 mM DTT. The assay mixture contained 50 μl of buffer (50 mM Tris-HCl, pH 7.8/20 mM KCl/5 mM $MgCl_2$/0.1 mM DTT), 250 μM sLLVY-MCA, and 50 μl of cell lysate (15 μg of protein). After 30 min at 37°C, the reaction was stopped by adding 1 ml of 0.2 M glycine buffer, pH 10, and the fluorescence of the liberated 7-amido-4-methylcoumarin was measured using the excitation and emission wavelengths at 365 and 460 nm, respectively.

Statistical analysis

Data are presented as mean ± SD. Comparisons between different treatments were performed using a Student's t-test. p values less than 0.05 were considered to be significant.

Results

H_2O_2 induces a bell-shaped nitric oxide signaling response

Endothelial cells were treated with different concentrations of GO (1–20 mU/ml). The rate of generation of H_2O_2 under these conditions varied from 0.05 μM/min to 1 μM/min [21]. Figure 1A shows the Western blots of phospho eNOS (phosphorylation at Ser1179), eNOS protein, phospho Akt and Akt induced in BAEC treated with a range of GO concentrations. Exposure to lower levels of GO (1–2 mU/ml) increased eNOS phosphorylation at Ser1179 (and not at Thr497) in BAEC, followed by a gradual decline in phospho eNOS induction in cells treated with increasing levels of GO (10–20 mU/ml). A similar trend was also noticed with total eNOS protein expression. These results are in agreement with the published report showing eNOS activation by a PI_3-kinase dependent phosphorylation at Ser1177 [5]. The present data indicate that H_2O_2 regulates Akt phosphorylation in a dose-dependent manner. As reported previously [5], we observed an increase in phosphoAkt (phosphorylated at Ser473) in BAEC treated with H_2O_2 generated at a lower rate, followed by a decrease in phosphoAkt expression in cells exposed to a higher rate of H_2O_2 generation. There was no detectable change in the total Akt levels under these conditions (Fig. 1A). These results suggest that treatment of endothelial cells with low levels of peroxide activate a unique signal transduction mechanism that was absent in cells treated with high peroxide levels.

Next we investigated whether changes in the phosphorylation status of eNOS protein parallel the increase in its activity. To this end, $^{\bullet}NO$ levels were examined, using different techniques, in cells exposed to varying H_2O_2 fluxes. Treatment with low GO levels (1–5 mU/ml) enhanced $^{\bullet}NO$ release in BAEC, as monitored by nitrate measurements in the medium (Fig. 1B), intracellular DAF-2-derived "green" fluorescence (Fig. 1C and D) and by HPLC analysis of intracellular DAF-2T product (Fig. 1E). All of these indicators of $^{\bullet}NO$ decreased considerably in cells treated with 20 mU/ml. Previously, it had been shown that DAF-2 forms a fluorescent triazole-type product in the presence of an oxidant derived from $^{\bullet}NO$ and oxygen interaction [37,38].

To investigate the effect of L-NAME (a non-specific inhibitor of all forms of NOS enzymes) on $^{\bullet}NO$ formation, BAEC were pretreated with L-NAME for 2 h and then treated with GO (2 mU/ml) for 4 h. As shown in Figure 2A and B, L-NAME pretreatment decreased the green fluorescence by about 20% in BAEC treated with 2 mU/ml of GO. In contrast, L-NAME pretreatment dramatically lowered the intracellular formation of DAF-2T, the characteristic marker product of DAF-2, $^{\bullet}NO$, and oxygen (Fig. 2C). Figure 2E shows the actual HPLC

chromatograms of the standards DAF-2 and DAF-2T and an unknown peak. The advantage of monitoring $^{\bullet}NO/DAF\text{-}2/O_2$ product by HPLC is that it enables us to monitor the intracellular uptake and metabolism of DAF-2DA. Although DAF-2 exhibits a much weaker fluorescent intensity (nearly three orders of magnitude less than DAF-2T), DAF-2 concentration in cells is nearly three orders of magnitude higher than that of DAF-2T. Thus, DAF-2 can contribute significantly to the intracellular fluorescence measured by microscopy. This may explain the much lower sensitivity to L-NAME of the fluorescence microscopy technique as compared to the HPLC assay. On the other hand the peak height due to DAF-2 is nearly identical during the various treatment conditions (Fig. 2E). This suggests that the observed changes in DAF-2T are not due to the differential cellular uptake of DAF-2DA. Figure 2D shows the levels of nitrate measured in the extracellular media under various conditions (Fig. 2A). We used the NOS inhibitor, L-NMMA instead of L-NAME, because L-NAME interfered with nitrate measurement by chemiluminescence. L-NMMA decreased the DAF-2 green fluorescence, albeit to a moderate extent (data not shown). These results suggest that DAF-2 green fluorescence, as monitored by fluorescence microscopy, could also originate by another oxidative route that is independent of $^{\bullet}NO$ formation under these conditions. As shown in Figure 2E, another green fluorescent product appeared at 4 min in the presence of 20 mU/ml GO. In contrast, DAF-2T measurement by HPLC in cells is more sensitive to changes in intracellular $^{\bullet}NO$ than the fluorescence microscopic technique.

H_2O_2 induces a bell-shaped proteolytic signaling response-Intermediacy of $^{\bullet}NO$

The proteasomal pathway is a major clearing route for damaged proteins, and failure of its function increases the accumulation of abnormal proteins [39]. The proteasomal function was assessed by measuring the activities of two of the most important proteasomal enzymes, chymotrypsin and trypsin. Both 26S and 20S proteasomal functions were measured in BAEC treated with a range of GO concentrations, as described previously [40]. GO treatment at concentrations ranging from 1–5 mU/ml significantly increased the proteasomal function (both 26 and 20S), whereas at a higher concentration (20 mU/ml) the proteasomal function significantly decreased (Figure 3A–B and 3C–D). Proteasomal activities were inhibited in the presence of L-NMMA or lactacystin. It was found that all these interventions could significantly prevent the proteasomal activation (26S and 20S) induced by 2mU/ml GO (Figure 4A–B and 4C–D). We independently confirmed this result by monitoring the proteasomal degradation of TfR in endothelial cells. Immunoblot studies using the antibody directed against TfR showed an accumulation of this protein in cells treated with a higher concentration of GO (20 mU/ml) and that this accumulation was not detected in cells treated with lower levels of GO (Figure 3E).

Lactacystin, a specific inhibitor of proteasome, was shown to induce eNOS expression in cells [41], and thus the effect of this inhibitor was investigated in cells exposed to 2 mU/ml of GO. As shown in Figure 2S in Supplementary Information, eNOS expression increased in the presence of 10 μM lactacystin and further increased with both lactacystin and 2 mU/mL GO. Functional $^{\bullet}NO$ was also detected under these conditions by measuring the DAF-2T product and nitrate release (Figure 2S).

Time-dependent $^{\bullet}NO$ and proteosomal activation in BAEC treated with GO

BAEC were treated with both low and high (2 mU/ml and 20 mU/ml) concentrations of GO for different time points ranging from 2–24 h, and $^{\bullet}NO$ and proteasome activities were measured. As shown in Figure 5, nitrate (A), DAF-2T (B), and eNOS (E) levels were elevated up to 8 h and maintained this level even at 24 h in BAEC exposed to GO (2 mU/ml), and nitrate and DAF-2T but not eNOS protein decreased at 24 h. In contrast, there was a significant decrease after 2 h in eNOS expression, nitrate and DAF-2T levels in cells treated with 20 mU/ml of GO during the same time period. Both 26S and 20S proteasomal activities were increased

in BAEC treated with 2 mU at 2 h time point, and this increase was maintained for up to 24 h (Fig. 6A–D).

Effect of low versus high concentrations of H_2O_2 on endothelial cell viability and apoptosis

BAEC were treated with H_2O_2 at concentrations ranging from 1 to 20 mU/ml GO and the cell viability was assessed by the MTT assay. The cell viability was virtually not affected in cells exposed to low levels of GO (1–10 mU/ml), whereas almost 70% of the cells were not viable in the presence of a higher concentration of GO (20 mU/ml) (Fig. 7B). Under these conditions, the caspase-3 activity was measured, which was significantly elevated in cells treated with 20 mU/ml of GO (Fig. 7A). Apoptosis was further confirmed by measuring DNA fragmentation using the TUNEL assay (Fig. 7C and D).

Discussion

In this work, we report that the exposure of endothelial cells to low concentrations of H_2O_2 stimulates •NO -mediated proteasomal signaling. There was, however, a decrease in •NO and proteasomal activation in cells treated with higher H_2O_2 fluxes. The fact that H_2O_2 induces a bell-shaped signaling response has important implications in endothelial cell survival and endothelial apoptosis induced by peroxides (Fig. 8).

Peroxide-induced endothelial NOS signaling

Previous studies have shown that exogenously-added H_2O_2 is a potent stimulator of •NO production in endothelial cells [5]. It was shown that both Ca^{2+} and calmodulin kinase II were involved in the signaling cascade linking H_2O_2 to eNOS induction [23]. More recently, endogenous levels of H_2O_2 generated in response to pathophysiological stimulus, angiotensin II, was reported to be sufficient to stimulate endothelial •NO formation [42]. The NADP(H) oxidase was shown to be responsible for angiotensin II-mediated H_2O_2 formation. Induction of eNOS by H_2O_2 was postulated as an important response to vascular oxidative stress [42].

H_2O_2-induced proteasomal function: Role of •NO

Recently, we reported that the •NO/cGMP/cAMP pathway can directly upregulate immunoproteasomal subunits (LMP2 and LMP7), thereby stimulating the proteasomal activities in endothelial cells [15]. Proteasomal activities were increased in BAEC treated with an •NO donor or with cell-permeable analogs of cGMP or cAMP. This increase in proteasomal activity was inhibited by specific adenylyl and guanylyl cyclase inhibitors [15]. Cells pretreated with protein kinase G and protein kinase A inhibitors markedly decreased •NO -dependent proteasome activation. The •NO/cGMP/cAMP signaling mechanism enhanced the phosphorylation of the transcription factor cAMP-response element-binding (CREB) protein, the cAMP-response element promoter activity and the expression of the immunoproteasomal subunits. In the present work, low levels of H_2O_2 induce •NO -dependent proteasomal activation. The regulatory mechanisms by which low levels of H_2O_2 upregulate proteasomal activities are proposed to be similar to the •NO -mediated signaling pathway. •NO as a stimulator of proteasomal function is an emerging concept [15]. The antioxidative and cytoprotective effects of •NO were attributed to proteasomal activation, as proteasomal inhibitors counteracted •NO -induced proteasomal activation [15]. Previous studies have shown that pretreatment of cells with antioxidants increased •NO stimulation and proteasomal function [43]. This is attributed to a decrease in ROS (e.g., H_2O_2) that in turn stimulates NOS signaling.

Previously, we reported that treatment of endothelial cells with a higher flux of H_2O_2 using GO (20 mU/ml) increased the expression of TfR levels leading to enhanced iron uptake and cellular apoptosis [21]. We also reported that this oxidant-induced iron signaling was effectively antagonized by exogenously-added •NO donors [40]. This effect was attributed to

an increase in proteasomal activation and the subsequent degradation of TfR levels on the cell surface. The present data further strengthens our previous suggestion [40], in that a lower flux of H_2O_2 enhanced eNOS protein phosphorylation and $^{\bullet}NO$ -mediated proteasomal activation. This process, in turn, regulates the accumulation of the oxidatively-modified proteins (e.g., TfR). However, in the presence of a higher flux of H_2O_2 the proteasomal activities were decreased, leading to increased accumulation of modified proteins and cell death.

Although the exact mechanism by which higher flux of H_2O_2 inhibits proteasome is not known, it is likely that this may be due to an increase in phosphatases activity resulting in eNOS dephosphorylation. Preliminary data indicate that okadaic acid reversed the proteasomal inactivation observed at higher flux of H_2O_2 (data not shown). Additional experiments are needed to fully explain these effects.

A bell-shaped response in redox biology

There exist several examples in oxidative pathophysiology where a bell-shaped dose-response was observed with respect to changes in the levels of antioxidant enzymes and antioxidant enzyme mimetics [44–46]. Early on, it was shown that MnSOD exhibited a bell-shaped dose-response in its protection against ischemic injury in isolated rabbit heart [44,45]. The bell-shaped dose-response behavior of SOD was invoked to explain the paradoxical over-production of protein carbonyls in cells with varying amounts of SOD [47]. As H_2O_2 is formed as an end-product in most pathophysiological processes, the bell-shaped cell signaling response reported for H_2O_2 could have major implications in understanding the cytotoxic and cytoprotective mechanisms of antioxidant enzymes and antioxidant enzyme mimetics in disease models. Biphasic redox-signaling was demonstrated in endothelial cells treated with ceramides [43]. Ceramides, a group of naturally occurring sphingolipid second messenger molecules, induce both $^{\bullet}NO$ and ROS in endothelial cells [43]. Lower levels of ceramide (5–20 μM) induced $^{\bullet}NO$ generation, whereas exposure to higher concentrations (>20 μM) induced ROS in endothelial cells. $^{\bullet}NO$ stimulation in endothelial cells exposed to lower concentrations of ceramide was attributed to Ca^{2+} activation and translocation of eNOS [14]. Antioxidants such as Mito-Q enhanced $^{\bullet}NO$ -mediated effects (i.e., proteasomal function) in BAEC treated with lower concentrations of ceramide [43]. Under these conditions, it is likely that ceramide effects were mediated through a biphasic ROS signaling [43]. More recently, superoxide was shown to counteract the signaling effects mediated by $^{\bullet}NO$ [48].

Finally, we report in this study that although DAF-2T (the authentic product of the reaction between DAF-2, $^{\bullet}NO$, and molecular oxygen) exhibits a characteristic green fluorescence, DAF-2 is also oxidatively converted to other green fluorescent products *via* a $^{\bullet}NO$ -independent mechanism. In addition, DAF-2 itself can contribute significantly to the intracellular green fluorescence (despite its much lower fluorescence quantum yield) due to its enhanced intracellular concentration as compared to DAF-2T. Consequently, the HPLC-fluorescence is a more reliable method for identification and quantitation of DAF-2T, the product of $^{\bullet}NO/O_2$ reaction with DAF-2.

Supplementary Material

Refer to Web version on PubMed Central for supplementary material.

Acknowledgments

This work was supported by NIH Grants RO1HL073056 and PO1HL68769.

References

1. Wolin S. Reactive oxygen species and vascular signal transduction mechanisms. Microcirculation 1996;3:1–17. [PubMed: 8846267]
2. Cai H, Harrison DG. Endothelial dysfunction in cardiovascular diseases: the role of oxidant stress. Circ Res 2000;87:840–844. [PubMed: 11073878]
3. Griendling KK, Harrison DH. Dual role of reactive oxygen species in vascular growth. Circ Res 1999;85:562–563. [PubMed: 10488060]
4. Carmody JR, Cotter TG. Signalling apoptosis: a radical approach. Redox Rep 2001;6:77–88. [PubMed: 11450987]
5. Thomas SR, Chen K, Keaney JF Jr. Hydrogen peroxide activates endothelial nitric-oxide synthase through coordinated phosphorylation and dephosphorylation via a phosphoinositide 3-kinase-dependent signaling pathway. J Biol Chem 2002;277:6017–6024. [PubMed: 11744698]
6. Rao GN, Berk BC. Active oxygen species stimulate vascular smooth muscle cell growth and proto-oncogene expression. Circ Res 1992;70:593–599. [PubMed: 1371430]
7. Baas AS, Berk BC. Differential activation of mitogen-activated protein kinases by H_2O_2 and O_2- in vascular smooth muscle cells. Circ Res 1995;77:29–36. [PubMed: 7540516]
8. Li P-F, Dietz R, von Harsdorf R. Differential effect of hydrogen peroxide and superoxide anion on apoptosis and proliferation of vascular smooth muscle cells. Circulation 1997;96:3602–3609. [PubMed: 9396461]
9. Patterson C, Madamanchi NR, Runge MS. The oxidative paradox: another piece in the puzzle. Circ Res 2000;87:1074–1076. [PubMed: 11110759]
10. Grune T, Davies KJ. The proteasomal system and HNE-modified proteins. Mol Aspects Med 2003;24:195–204. [PubMed: 12892997]
11. Finkel T. Oxidant signals and oxidative stress. Curr Opinion Cell Biol 2003;15:247–254. [PubMed: 12648682]
12. Wood ZA, Poole LB, Karplus PA. Peroxiredoxin evolution and regulation of hydrogen peroxide signaling. Science 2003;300:650–653. [PubMed: 12714747]
13. Drummond GR, Cai H, Davis ME, Ramasamy S, Harrison DG. Transcriptional and posttranscriptional regulation of endothelial nitric oxide synthase expression by hydrogen peroxide. Circ Res 2000;86:347–354. [PubMed: 10679488]
14. Igarashi J, Thatte HS, Prabhakar P, Golan DE, Michel T. Calcium-independent activation of endothelial nitric oxide synthase by ceramide. Proc Natl Acad Sci U S A 1999;96:12583–12588. [PubMed: 10535965]
15. Kotamraju S, Matalon S, Matsunaga T, Shang T, Hickman-Davis JM, Kalyanaraman B. Upregulation of immmunoproteasomes by nitric oxide: potential antioxidative mechanism in endothelial cells. Free Radic Biol Med 2006;40:1034–1044. [PubMed: 16540399]
16. Ross R. The pathogenesis of atherosclerosis: a perspective for the 1990s. Nature 1993;362:801–809. [PubMed: 8479518]
17. Alexander RW. Hypertension and the pathogenesis of atherosclerosis. Oxidative stress and the mediation of arterial inflammatory response: a new perspective. Hypertension 1995;25:155–161. [PubMed: 7843763]
18. Ross R. The pathogenesis of atherosclerosis: an update. N Engl J Med 1986;314:488–500. [PubMed: 3511384]
19. Hwang J, Saha A, Boo YC, Sorescu GP, McNally JS, Holland SM, Dikalov S, Giddens DP, Griendling KK, Harrison DG, Jo H. Oscillatory shear stress stimulates endothelial production of O_2- from p47phox-dependent NAD(P)H oxidases, leading to monocyte adhesion. J Biol Chem 2003;278:47291–47298. [PubMed: 12958309]
20. Hwang J, Ing MH, Salazar A, Lassegue B, Griendling K, Navab M, Sevanian A, Hsiai TK. Pulsatile versus oscillatory shear stress regulates NADPH oxidase subunit expression: implication for native LDL oxidation. Circ Res 2003;93:1225–1232. [PubMed: 14593003]
21. Tampo Y, Kotamraju S, Chitambar CR, Kalivendi SV, Keszler A, Joseph J, Kalyanaraman B. Oxidative stress-induced iron signaling is responsible for peroxide-dependent oxidation of dichlorodihydrofluorescein in endothelial cells. Circ Res 2003;92:56–63. [PubMed: 12522121]

22. Cai H, Li Z, Dikalov S, Holland SM, Hwang J, Jo H, Dudley SC Jr, Harrison DG. NAD(P)H oxidase-derived hydrogen peroxide mediates endothelial nitric oxide production in response to angiotensin II. J Biol Chem 2002;277:48311–48317. [PubMed: 12377764]

23. Cai H, Davis ME, Drummond GR, Harrison DG. Induction of endothelial NO synthase by hydrogen peroxide via a Ca^{2+}/calmodulin-dependent protein kinase II/Janus kinase 2-dependent pathway. Atheroscler Thromb Vasc Biol 2001;21:1571–1576.

24. Wink DA, Hanbauer I, Krishna MC, DeGraff W, Gamson J, Mitchell JB. Nitric oxide protects against cellular damage and cytotoxicity from reactive oxygen species. Proc Natl Acad Sci U S A 1993;90:9813–9817. [PubMed: 8234317]

25. Beltran B, Mathur A, Duchen MR, Erusalimsky JD, Moncada S. The effect of nitric oxide on cell repiration: a key to understanding its role in cell survival or death. Proc Natl Acad Sci U S A 2000;97:14602–14607. [PubMed: 11121062]

26. Rubbo H, Parthasarthy S, Barnes S, Kirk M, Kalyanaraman B, Freeman BA. Nitric oxide inhibition of lipoxygenase-dependent liposome and low-density lipoprotein oxidation: termination of radical chain propogation reactions and formation of nitrogen-containing oxidized lipid derivatives. Arch Biochem Biophys 1995;324:15–25. [PubMed: 7503550]

27. Landmesser U, Dikalov S, Price SR, McCann L, Fukai T, Holland SM, Mitch WE, Harrison DG. Oxidation of tetrahydrobiopterin leads to uncoupling of endothelial cell nitric oxide synthase in hypertension. J Clin Invest 2003;111:1201–1209. [PubMed: 12697739]

28. Hayon T, Dvilansky A, Shpilberg O, Nathan I. Appraisal of the MTT-based assay as a useful tool for predicting drug chemosensitivity in leukemia. Leuk Lymphoma 2003;44:1957–62. [PubMed: 14738150]

29. Kotamraju S, Hogg N, Joseph J, Keefer LK, Kalyanaraman B. Inhibition of oxidized low-density lipoprotein-induced apoptosis in endothelial cells by nitric oxide: peroxyl radical scavenging as an antiapoptotic mechanism. J Biol Chem 2001;276:17316–17323. [PubMed: 11278975]

30. Kotamraju S, Chitambar CR, Kalivendi SV, Joseph J, Kalyanaraman B. Transferrin receptor-dependent iron uptake is responsible for doxorubicin-mediated apoptosis in endothelial cells. J Biol Chem 2002;277:17179–17187. [PubMed: 11856741]

31. Kojima H, Nakatsubo N, Kikuchi K, Kawahara S, Kirino Y, Nagoshi H, Hirata Y, Nagano T. Detection and imaging of nitric oxide with novel fluorescent indicators: diaminofluoresceins. Anal Chem 1998;70:2446–2453. [PubMed: 9666719]

32. Rodriguez J, Specian V, Maloney R, Jourd'heuil D, Feelisch M. Performance of diamino fluorophores for the localization of sources and targets of nitric oxide. Free Radic Biol Med 2005;38:356–368. [PubMed: 15629864]

33. Miranda KM, Espey MG, Wink DA. A rapid, simple spectrophotometric method for simultaneous detection of nitrate and nitrite. Nitric Oxide 2001;5:62–71. [PubMed: 11178938]

34. Coux O, Tanaka K, Goldberg AL. Structure and functions of the 20S and 26S proteasomes. Ann Rev Biochem 1996;65:801–847. [PubMed: 8811196]

35. Pajonk F, Riess K, Sommer A, McBride WH. N-acetyl-L-cysteine inhibits 26S proteasome function: implications for effects on NF-kappaB activation. Free Radic Biol Med 2002;32:536–543. [PubMed: 11958954]

36. Grune T, Reinheckel T, Davies KJ. Degradation of oxidized proteins in K562 human hematopoietic cells by proteasome. J Biol Chem 1996;271:15504–15509. [PubMed: 8663134]

37. Espey MG, Thomas DD, Miranda KM, Wink DA. Focusing of nitric oxide mediated nitrosation and oxidative nitrosylation as a consequence of reaction with superoxide. Proc Natl Acad Sci U S A 2002;99:11127–11132. [PubMed: 12177414]

38. Tarpey MM, Wink DA, Grisham MB. Methods for detection of reactive metabolites of oxygen and nitrogen: in vitro and in vivo considerations. Am J Physiol Regul Integ Comp Physiol 2004;286:R431–344.

39. Taylor A, Davies KJA. Protein oxidation and loss of protease activity may lead to cataract formation in the aged lens. Free Radic Biol Med 1987;3:371–377. [PubMed: 3322949]

40. Kotamraju S, Tampo Y, Keszler A, Chitambar CR, Joseph J, Haas AL, Kalyanaraman B. Nitric oxide inhibits H_2O_2-induced transferrin receptor-dependent apoptosis in endothelial cells: Role of

ubiquitin-proteasome pathway. Proc Natl Acad Sci U S A 2003;100:10653–10658. [PubMed: 12958216]

41. Stangl V, Lorenz M, Meiners S, Ludwig A, Bartsch C, Moobed M, Vietzke A, Kinkel HT, Baumann G, Stangl K. Long-term up-regulation of eNOS and improvement of endothelial function by inhibition of the ubiquitin-proteasome pathway. FASEB J 2004;18:272–279. [PubMed: 14769821]
42. Cai H, Li Z, Dikalov S, Holland SM, Hwang J, Jo H, Dudley SC Jr, Harrison DG. NAD(P)H oxidase-derived hydrogen peroxide mediates endothelial nitric oxide production in response to angiotensin II. J Biol Chem 2002;277:48311–48317. [PubMed: 12377764]
43. Matsunaga T, Kotamraju S, Kalivendi SV, Dhanasekaran A, Joseph J, Kalyanaraman B. Ceramide-induced intracellular oxidant formation, iron signaling, and apoptosis in endothelial cells. J Biol Chem 2004;279:28614–28624. [PubMed: 15102832]
44. Nelson SK, Bose SK, McCord JM. The toxicity of high-dose superoxide dismutase suggests that superoxide can both initiate and terminate lipid peroxidation in the reperfused heart. Free Radic Biol Med 1994;16:195–200. [PubMed: 8005514]
45. Galiñanes M, Ferrari R, Qiu Y, Cargnoni A, Ezrin A, Hearse DJ. PEG-SOD and myocardial antioxidant status during ischaemia and reperfusion: Dose-response studies in the isolated blood perfused rabbit heart. J Mol Cell Cardiol 1992;24:1021–1030. [PubMed: 1433318]
46. Offer T, Russo A, Samuni A. The pro-oxidative activity of SOD and nitroxide SOD mimetics. FASEB J 2000;14:1215–1223. [PubMed: 10834943]
47. Lushchak V, Semchyshyn H, Lushchak O, Mandryk S. Diethyldithiocarbamate inhibits in vivo Cu, Zn-superoxide dismutase and perturbs free radical processes in the yeast *Saccharomyces cerevisiae* cells. Biochem Biophys Res Commun 2005;338:1739–1744. [PubMed: 16274662]
48. Thomas DD, Ridnour LA, Espey MG, Donzelli S, Ambs S, Hussain SP, Harris CC, DeGraff W, Roberts DD, Mitchell JB, Wink DA. Superoxide Fluxes Limit Nitric Oxide-induced Signaling. J Biol Chem 2006;281:25984–25993. [PubMed: 16829532]

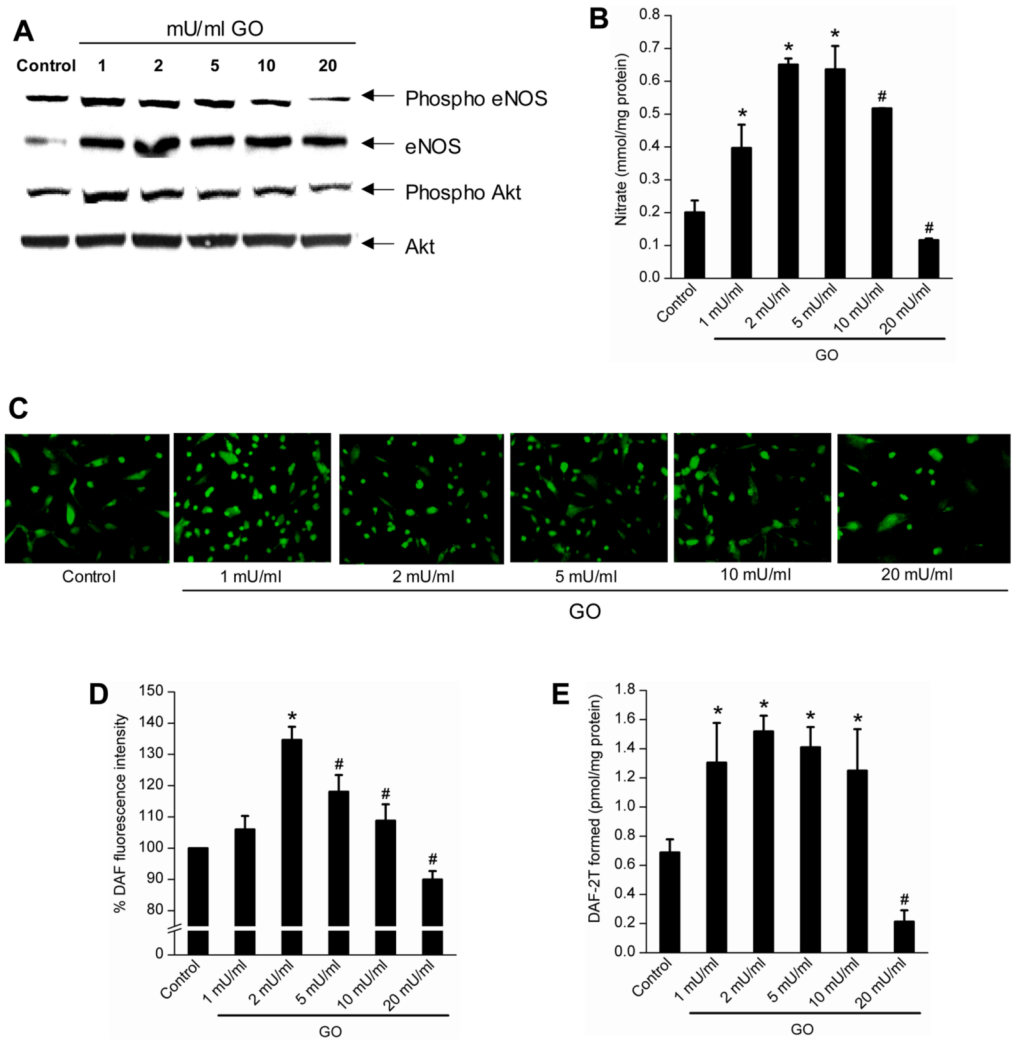

Figure 1.

Dose-dependent effects of H_2O_2 on eNOS and Akt phosphorylations and •NO generation in BAEC treated with Glu/GO. **A,** BAEC were treated with different concentrations of GO for 4 h, and cell lysates probed with anti-phospho eNOS, eNOS, phospho Akt, and total Akt antibodies as described in *Materials and Methods.* **B,** Cells were treated as in **A** and the culture media analyzed for nitrate levels. **C,** Fluorescence micrographs obtained from cells treated as in **A** followed by a treatment with 5 μM DAF-2DA as described in *Materials and Methods.* **D,** Densitometric analysis of the fluorescence data shown in **C**. The control fluorescence intensity was normalized to 100%. **E,** DAF-2-triazole extracted from BAEC treated with varying concentrations of GO as in **C**. DAF-2-triazole was measured by HPLC as described in *Materials and Methods.* * $p < 0.05$ as compared to control; # $p < 0.05$ as compared to 2 mU/ml GO sample.

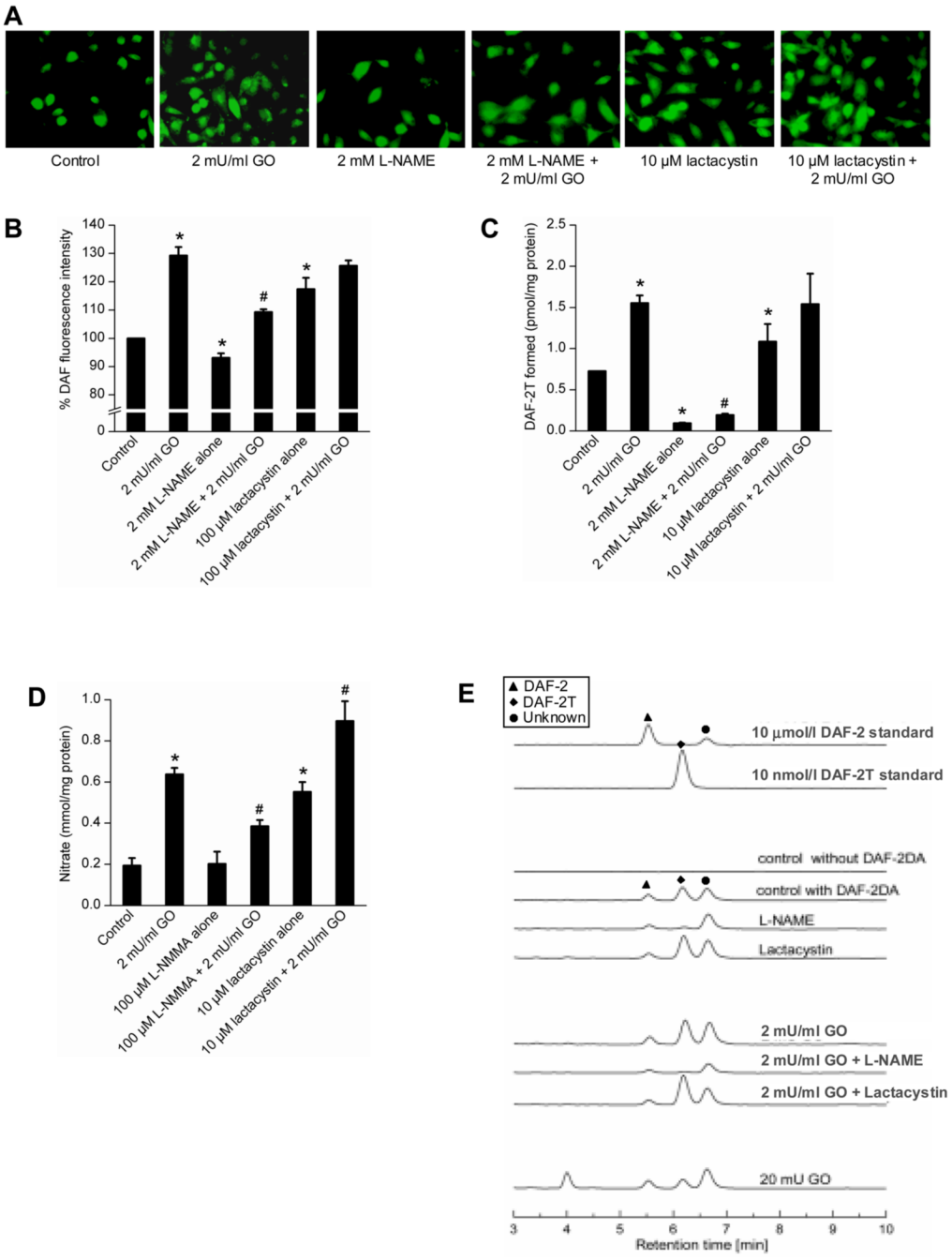

Figure 2.

The effect of L-NAME and lactacystin on H_2O_2-induced DAF-2 fluorescence and DAF-2T formation. **A,** BAEC were treated with GO (2 mU/ml) for 4 h with and without L-NAME and lactacystin pretreatment and fluorescent micrographs obtained after treatment with DAF-2DA. **B,** Same as **A** except that the graph shows the densitometric analysis of the fluorescence data shown in **A**. The control fluorescence intensity was taken as 100%. **C,** DAF-2T formation as measured by HPLC from cells treated under conditions shown in **A. D,** Graph showing nitrate levels measured in the cell culture media following treatment of cells as in **A** but in the absence of DAF-2DA. **E,** HPLC traces of DAF-2 and DAF-2T standards, n-butanol extracts of control and GO-treated cells with and without pretreatment of L-NAME and lactacystin as shown in

A. Symbols marked in the HPLC traces represent the species, as shown in the inset. * $p < 0.05$ as compared to control; # $p < 0.05$ as compared to 2 mU/ml GO sample..

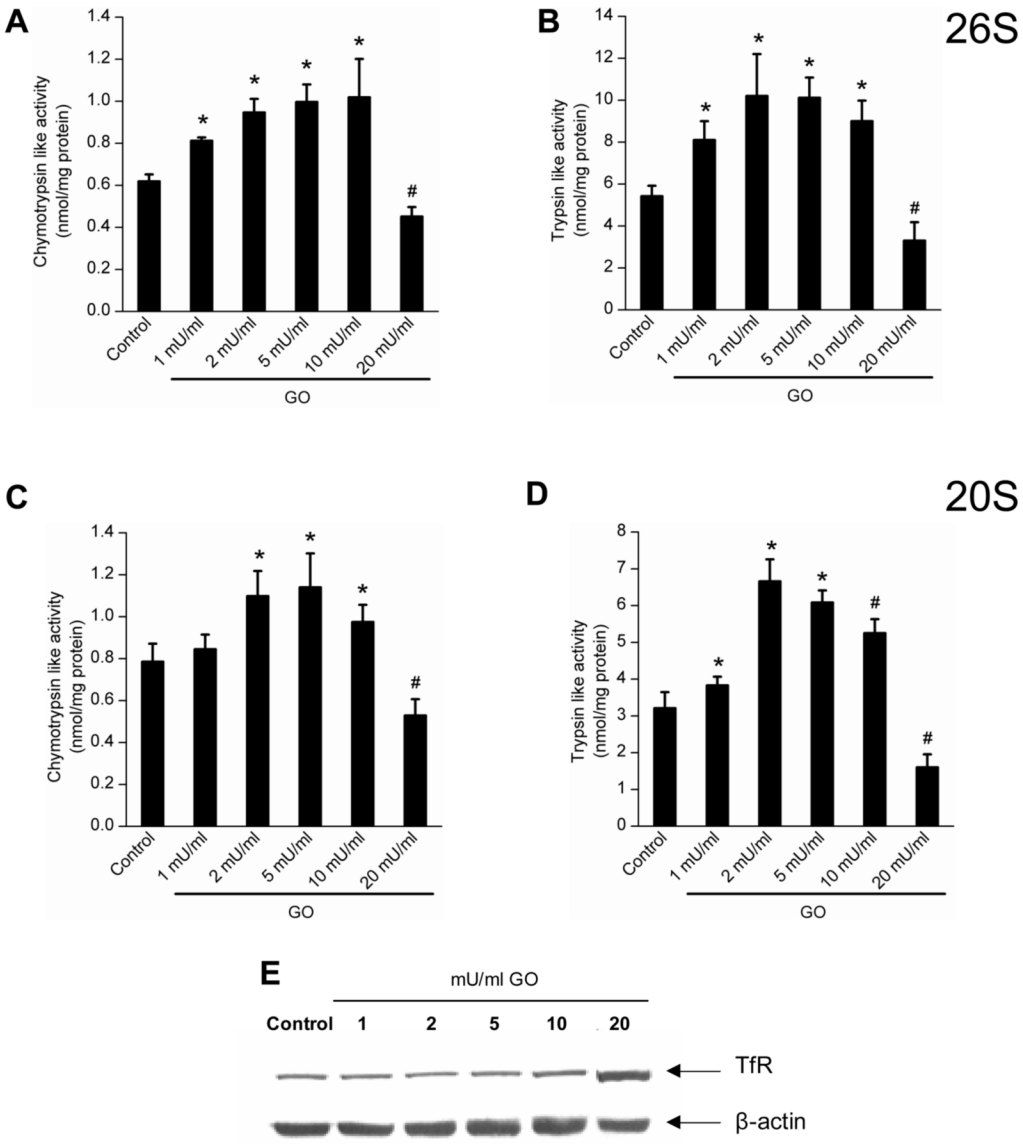

Figure 3.

Dose-dependent effects of GO on proteasomal function. **A** and **B,** BAEC were treated with different concentrations of GO (1–20 mU/ml) for 4 h, and chymotrypsin- and trypsin-like activities of 26S proteosome measured as described in *Materials and Methods*. **C** and **D,** Treatment conditions same as above and the chymotrypsin and trypsin-like activities of 20S proteasome were measured. **E,** Western blot of transferrin receptor protein levels monitored in cell lysates of BAEC after treatment with GO (1–20 mU/ml). * $p < 0.05$ as compared to control; # $p < 0.05$ as compared to 2 mU/ml GO sample.

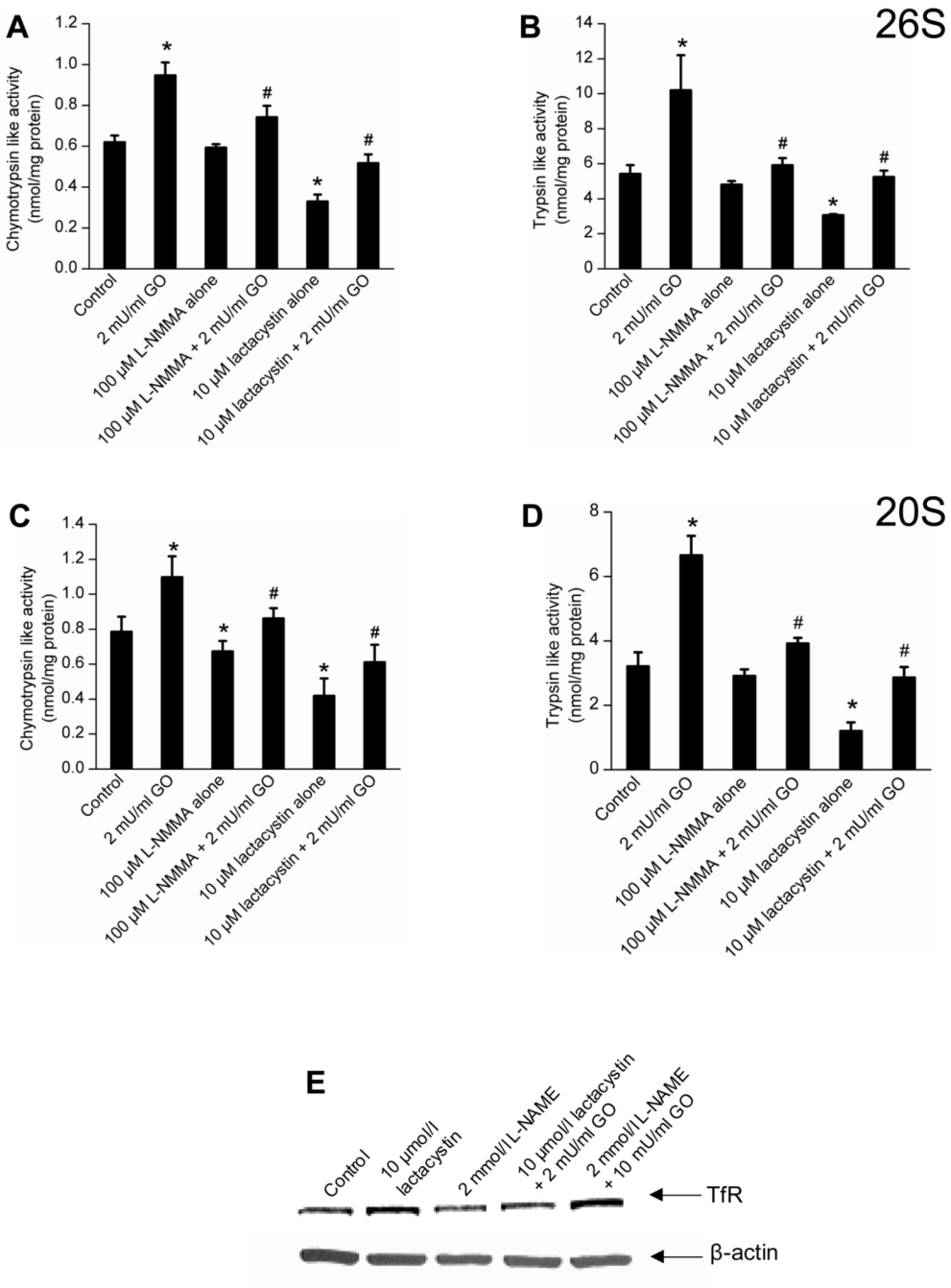

Figure 4.

The effects of NOS and proteasome inhibitors on proteasomal activation in BAECs treated with low levels of GO. **A** and **B,** BAEC were treated for 4 h with GO (2 mU/ml) before and after pretreatment with L-NMMA and lactacystin for 2 h. The graphs show the chymotrypsin- and trypsin-like activities of 26S proteasome measured under different treatment conditions. **C** and **D,** Same as above, except the chymotrypsin- and trypsin-like activities of 20S proteasome were measured. **E,** The Western blot of TfR protein levels was measured following the same treatment conditions as described above. * $p < 0.05$ as compared to control; # $p < 0.05$ as compared to 2 mU/ml GO sample.

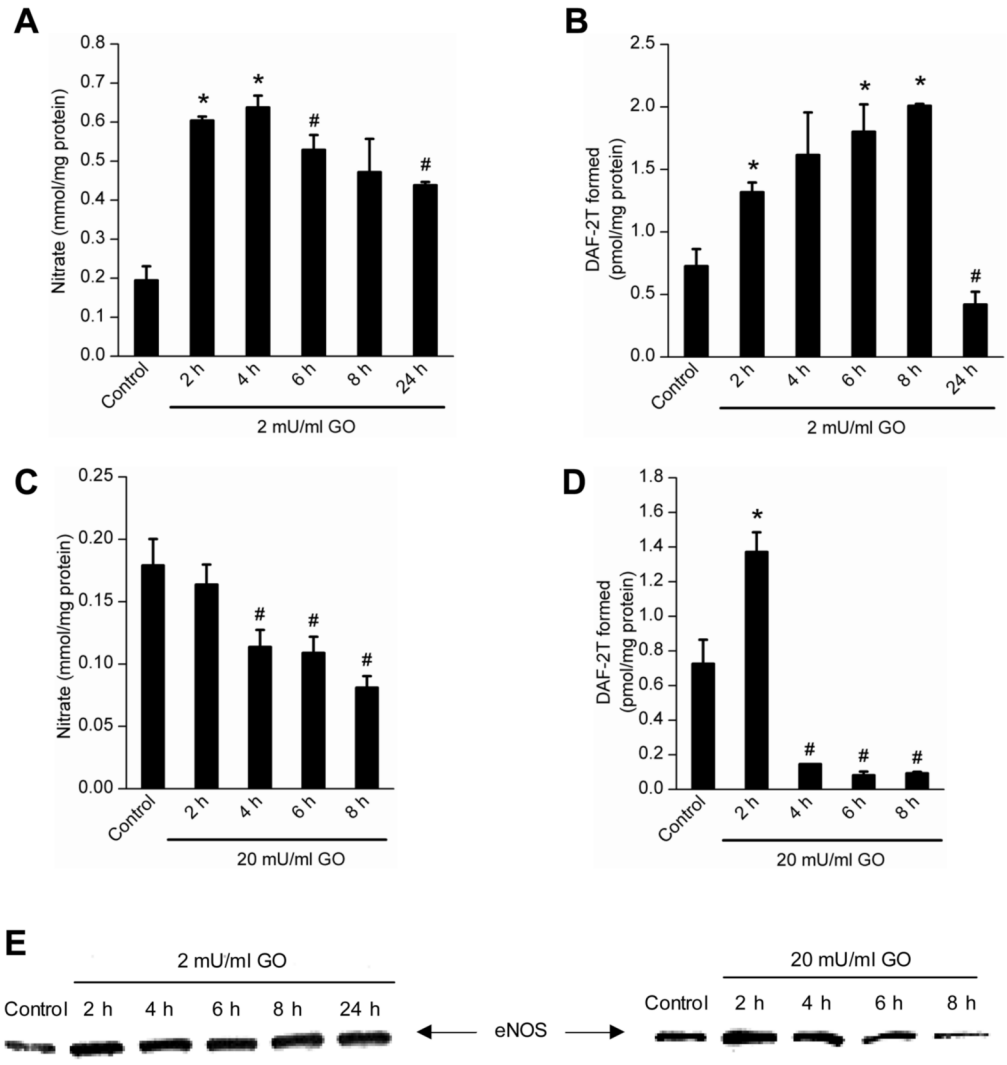

Figure 5.

Measurements of nitrate and DAF-2T in cells treated with low and high levels of GO. **A** and **B,** BAEC were treated with 2 mU/ml of GO for different time periods and nitrate release (**A**) and intracellular DAF-2T levels (**B**) were measured. **C** and **D,** Same as above, except that cells were treated with GO (20 mU/ml) and nitrate (**C**) and DAF-2T (**D**) measured as described in *Materials and Methods.* **E,** Immunoblots of eNOS protein measured in cell lysates after treatment with 2 and 20 mU/ml of GO. * $p < 0.05$ as compared to control; # $p < 0.05$ as compared to 4 h (**A**), 6 h (**B**) and 2 h (**C** and **D**) incubation with GO.

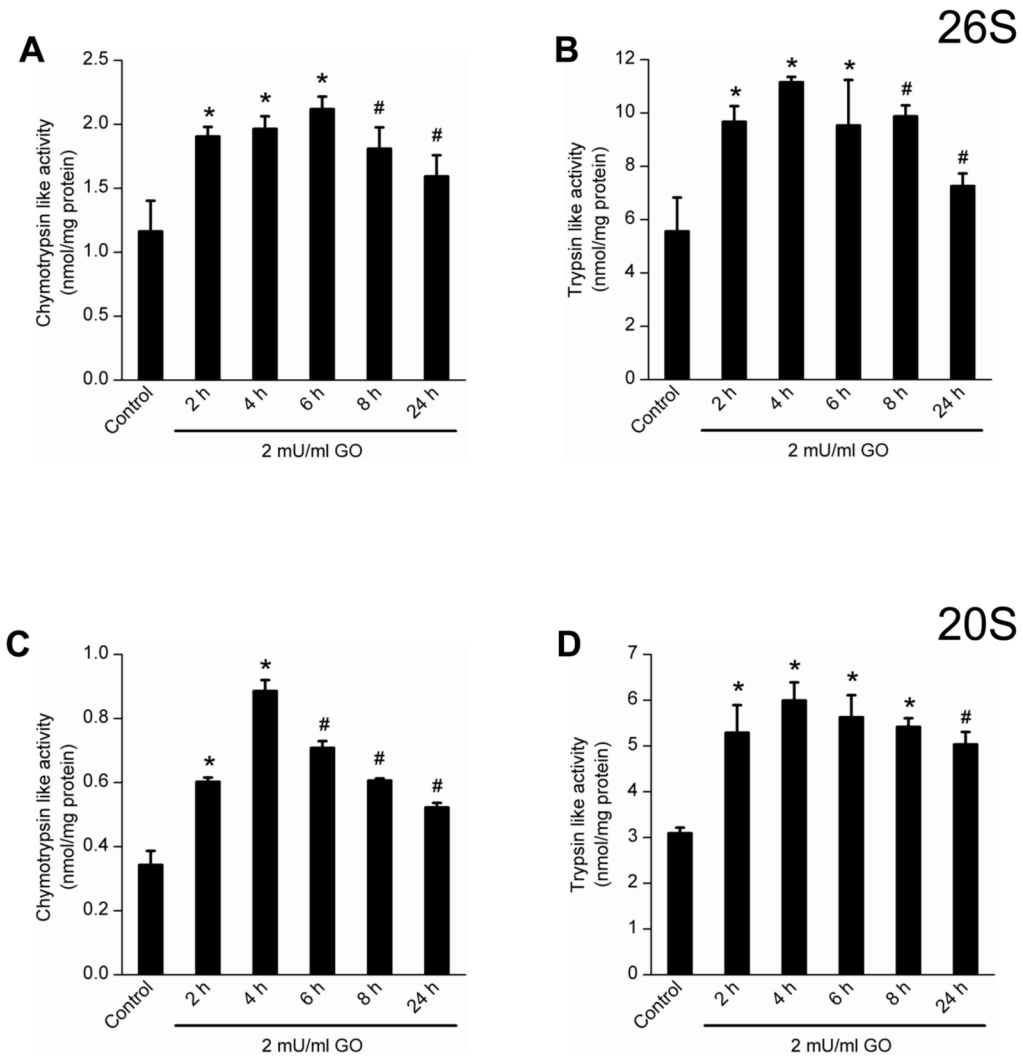

Figure 6.

Time-dependent changes in proteasome activity in BAEC treated with low dose of GO. **A** and **B,** BAEC were treated with 2 mU/ml for different time periods as shown, and the chymotrypsin- and trypsin-like activities of 26S proteasome measured in cell lysates. **C** and **D,** Same as above, except that the chymotrypsin- and trypsin-like activities of 20S proteasome were measured in cell lysates. * $p < 0.05$ as compared to control; # $p < 0.05$ as compared to 6 h (**A**), and 4 h (**B**, **C** and **D**) incubation with GO.

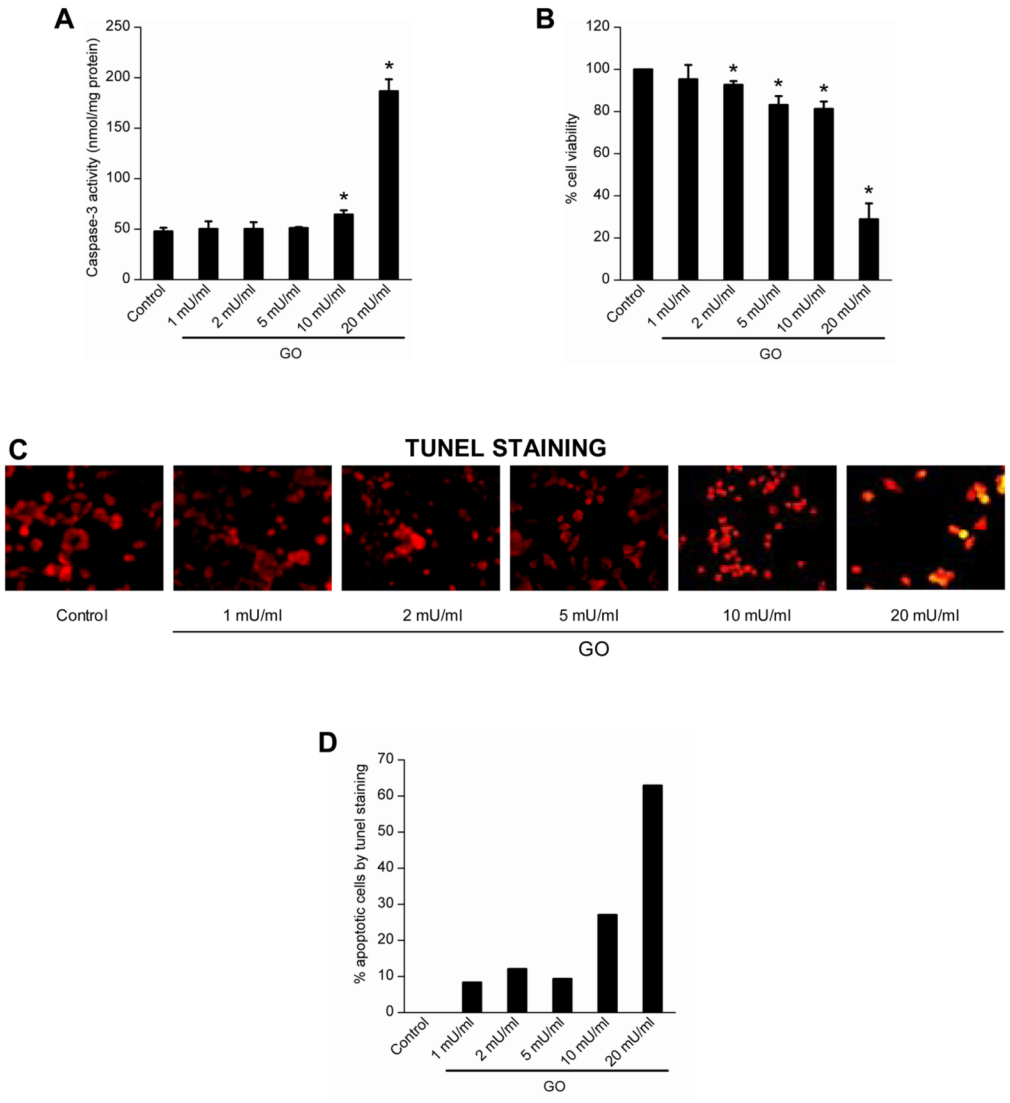

Figure 7.

Dose-dependent effects of GO on endothelial apoptosis. **A,** BAEC were treated with GO (1–20 mU/ml) for 8 h, and the caspase-3 activity measured by monitoring the release of p-nitroanilide. **B,** Treatment conditions same as above and the cell viability was measured by the MTT assay. **C,** Treatment conditions same as in **A** and cells stained for TUNEL-positive cells and examined by fluorescence microscopy. Photographs are overlaid images of propidium iodide and FITC-stained cells. Apoptotic and non-apoptotic cells are denoted by yellow and red colors. **D,** Treatment conditions same as **A** and the graph shows the percent of TUNEL-positive cells in response to different treatment conditions. * $p < 0.05$ as compared to control.

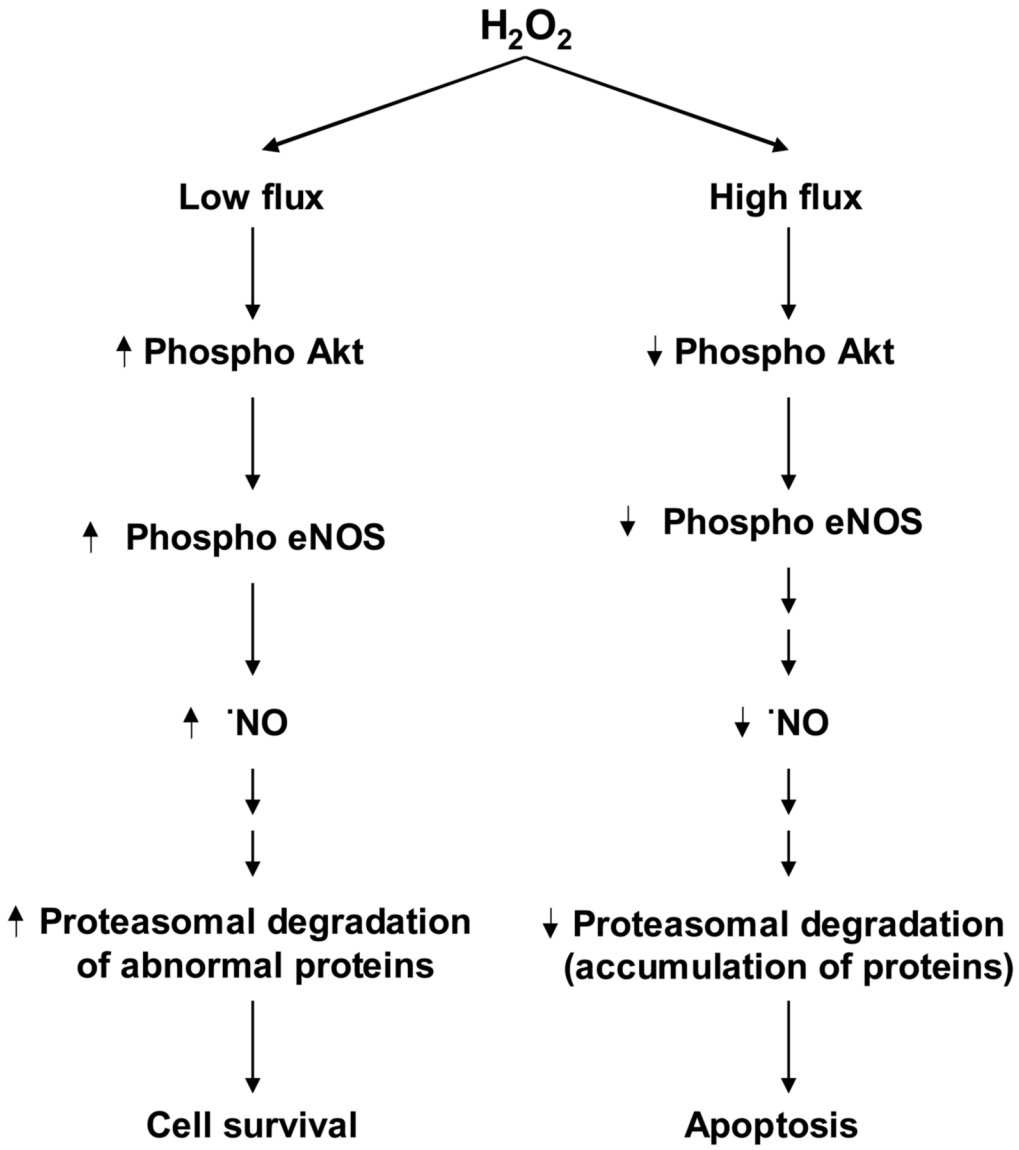

Figure 8.
Nitric oxide mediated regulation of proteasomal function in response to H_2O_2-induced endothelial cell survival and cell death.